

Original hybrid control for robotic structures using Magnetic Shape Memory Alloys actuators

Jean-Yves Gauthier, Arnaud Hubert, Joël Abadie, Nicolas Chaillet and Christian LExcellent

Abstract—Magnetic Shape Memory Alloys (MSMA) are relatively new active materials but at this time they are not actually very used as actuators despite a high strain and a small response time. This is probably due in part to a large hysteresis and a strong non-linear behaviour. In this paper, an original hybrid control is designed taking into account dynamical effects and hysteretic behaviour in order to increase static gain of the system. After a short presentation of MSMA behaviour, a modelling is proposed to obtain two different control strategies. Some experimental results are also given.

Index Terms—control, active material, adaptronic, Magnetic Shape Memory Alloy, nonlinear, dynamics, hysteresis.

I. INTRODUCTION

In mechatronic field and specially micro-mechatronic, active materials are mostly used as actuators. Among these, Magnetic Shape Memory Alloys (MSMA) present interesting properties: they permit high reachable strain (about 6 to 10 %) as classical Shape Memory Alloys (SMA), but with a very smaller time response (a few ms) [1], [2], [3]. From a control engineer point of view, this material opens new possibilities. Nevertheless, the very large hysteresis of this material in addition to its small response time implies the need of new control laws design. An other problem of the MSMA is the high magnetic field to initiate strain (or displacement). In this paper, we propose two hybrid controls of an experimental system we developed that permit a large displacement range with small electrical currents by using dynamical effects of the load. In the section II, the MSMA actuation as well as the experimental system are presented. A modelling is then established in the section III including an energy discussion. Hybrid control strategies are introduced and used on an experimental test bench in the section IV. Finally, perspectives are envisaged in the fields of micro-positioning and micro-robotics.

II. SYSTEM PRESENTATION

A. Magnetic Shape Memory Alloys

The MSMA studied here is the most widespread Ni-Mn-Ga single crystal. Our samples come from the finnish company AdaptaMat Ltd. (<http://www.adaptamat.com/>). In this material, the martensite structure can appear in three

This work was supported by the French Education and Research Ministry and the French National Center for Scientific Research (CNRS)

J. Y. Gauthier, A. Hubert, J. Abadie and N. Chaillet are with the Laboratoire d'Automatique de Besançon, CNRS, ENSMM, UFC ; 24 rue Alain Savary, 25000 Besançon, France {jygauthi, ahubert, jabadie, chaillet}@ens2m.fr

Christian LExcellent is with the Institut Femto-st, CNRS, ENSMM, UFC, UTBM ; 24 chemin de l'Épitaphe, 25000 Besançon, France christian.lexcellent@univ-fcomte.fr

different orientations corresponding to the three martensite variants (cf. Fig. 1 (a)).

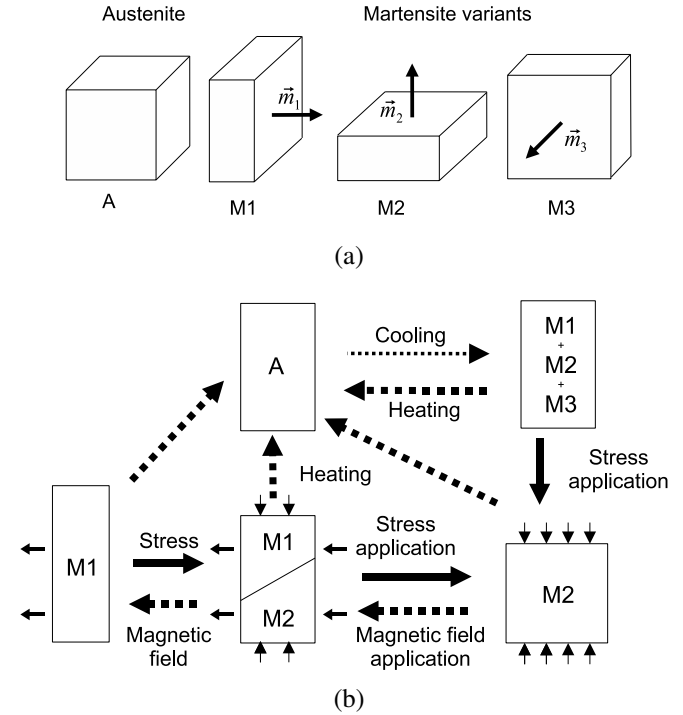


Fig. 1. MSMA behaviour: (a) austenite phase and the three martensite variants, (b) martensitic reorientation: effects of mechanical stress, magnetic field and temperature.

Martensitic reorientation principle is presented on Fig. 1 (b): at high temperature, MSMA sample is in austenitic phase. After cooling, the austenite is transformed into martensite without favouring any variants. The resulting sample contains therefore the martensite variants into three equal fractions (M1, M2 and M3). If a mechanical stress is applied in a specified direction, the variant with its short axis in the same direction is growing at the cost of others. If this stress is sufficient, the sample contains finally only this variant (for example M2 on Fig. 1 (b)). If the stress is decreasing, the volume fraction of M2 variant does not decrease seriously. In the same way, if a magnetic field is applied perpendicular to the stress field, variant M_i with its easy magnetization direction \vec{m}_i in the field direction is favoured. The easy magnetization direction corresponds to the short axis of the variant. As an example, the M1 variant (cf. Fig. 1 (b)) is increasing when a magnetic field is applied.

The balance between magnetic field and mechanical stress effects creates a controlled macroscopic strain of the martensite. Using a pre-stress, it permits to obtain an actuator driven by magnetic field.

One has to denote that austenite phase can be recovered by heating. This alloy has some drawbacks like brittleness, high magnetic field to create (400 kA/m), large dependence of material parameters on temperature changes, small blocking stress (2-3 MPa) and large hysteresis. A review and a comparison between smart materials including MSMA is available in [4].

B. System description

In this paper, MSMA behaviour is studied in a full system including a magnetic field generator and a mechanical load. This system is presented on Fig. 2: a magnetic circuit containing a coil and a ferromagnetic core permits to create a magnetic field in the air-gap where the MSMA sample is inserted. The latter is in mechanical contact at one extremity with the fixed support and at the other extremity with a mobile load. The weight of this load permits to pre-stress the MSMA sample and to obtain a motion in two ways. Inertial effects have to be taken into account. Response time of the mechanical load is about 25 ms. The coil is supplied by an home-made switching power amplifier (200 V - 2 A max) with a current control by feedback. The rise time from 0 to 1 A is about 3 ms. Displacement is measured with a laser sensor (Keyence LK-152). A DSP board (dSpace) is used to control the system with the help of Matlab/Simulink[®] and dSPACE[®] softwares.

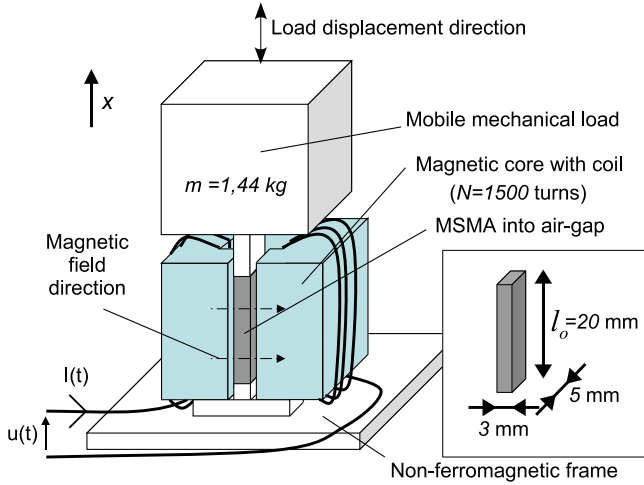


Fig. 2. General view of the system.

III. MODELLING

A. MSMA modelling

The MSMA modelling is based on the thermodynamics of irreversible processes with internal variables [5]. If we note z the M_1 martensite volume fraction, the strain can be expressed as:

$$\varepsilon = \frac{\sigma}{E} + \gamma z \quad (1)$$

Where E is the Young modulus of the material and γ is the total uniaxial detwinned strain. This parameter is obtained by a MSMA crystallographic study. σ is the stress applied on the MSMA sample. From a thermodynamics point of view, each variable q_i has an associated force F_i defined by:

$$F_i = -\frac{\partial G}{\partial q_i} \quad (2)$$

Where G is the MSMA Gibbs free energy. The force associated with the internal variable z is noted π_f^* . Moreover, if we neglect the interaction between the two martensite variants M_1 and M_2 , the thermodynamic force exerted on the volume fraction z is:

$$\pi_f^* = \gamma\sigma + \pi_f^{mag}(H) \quad (3)$$

$\pi_f^{mag}(H)$ is a function of the magnetic field H depending on the current i flowing into the coil. This current is driven by the power amplifier. The dynamic of the amplifier can be neglected in this paper because of its high bandwidth. Therefore, $\pi_f^{mag}(i)$ can be considered as the input control of our system. π_f^* is a function of z (see Fig. 3). In a first step, the hysteretical behaviour is taken into account with simple inner loops (Fig. 3 (a)) although the exact real behaviour must be considered with more complicated inner loops (Fig. 3 (b)).

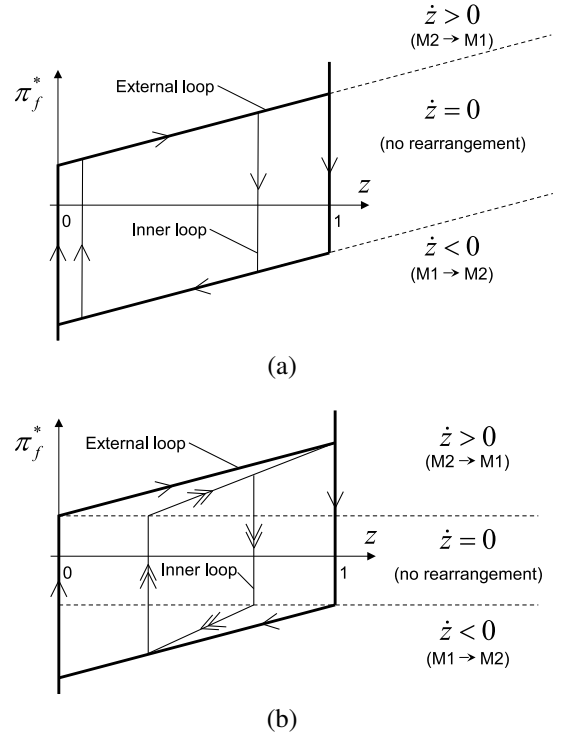


Fig. 3. Martensite volume fraction z as a function of its thermodynamical force π_f^* : (a) with simple inner loops, (b) with more complicated inner loops.

B. Load modelling

We assume that a contact between the load and the MSMA sample is always held:

$$\begin{aligned} F &= -\sigma S \\ x &= l_o \varepsilon \end{aligned} \quad (4)$$

where F is the force exerted on the surface S of the load, l_o the length of MSMA sample and x is the displacement of the load. The dynamics of the load follows the Newton Law:

$$m\ddot{x} = -mg - f\dot{x} + F \quad (5)$$

where f , g and m are, respectively, the viscous friction parameter, the standard gravity and the mass of the load.

C. Control issue

1) *Theoretical point of view*: by using (3), (4) and (5), we obtain:

$$\pi_f^* = \pi_f^{mag}(i) - \frac{mg\gamma}{S} - \frac{f\gamma}{S}\dot{x} - \frac{m\gamma}{S}\ddot{x} \quad (6)$$

The first term on the right side of (6) is the input control, the second one is a constant, the third term is proportional to the velocity \dot{x} and the fourth is proportional to the acceleration \ddot{x} . (1), (4) and (5) in static mode ($\dot{x} = \ddot{x} = 0$) give:

$$x = l_o \varepsilon = l_o \gamma z - \frac{l_o mg}{SE} \quad (7)$$

With $l_o = 20$ mm and $\gamma = 0.06$, the maximum displacement due to martensite reorientation, i.e. when z goes from 0 to 1, is $1200 \mu\text{m}$. We consider the case where the displacement is increasing ($\dot{x} > 0$), a similar extension for decreased displacement can be easily obtained. The aim of our control is to obtain a maximum static displacement x with a limited input range. Therefore, according to (7), z and so π_f^* have to be maximum to satisfy the control requirements. By using (6), the first term $\pi_f^{mag}(i)$ has to be maximum but is limited by the maximum current i_{max} . The second term of (6) stays constant. The third term can only be negative, so it could be interesting to minimize damping f in the system design in order to maximize π_f^* . The fourth term can be positive if the load slow down ($\ddot{x} < 0$) and so π_f^* can be increased by dynamical effects. This last way is shown on the following experimental tests.

2) *Experimental checking*: a current is set into the coil and the corresponding displacement is drawn on the Fig. 4. The maximum reachable displacement is larger when the current is applied quickly (dynamic mode) than when it is applied slowly (quasi-static mode).

x_{min}^S and x_{max}^S are the minimum and maximum reachable displacement values in quasi-static mode. These values depend on material strain history. In this paper, they are considered as constants, nevertheless, the control could be extended for the non-constant case. *Reset* sequence is always applied before any experiment to agree with the assumption of keeping constant these parameters. A_{max} and A_{min} are respectively the absolute maximum and minimum displacements reachable by the system.

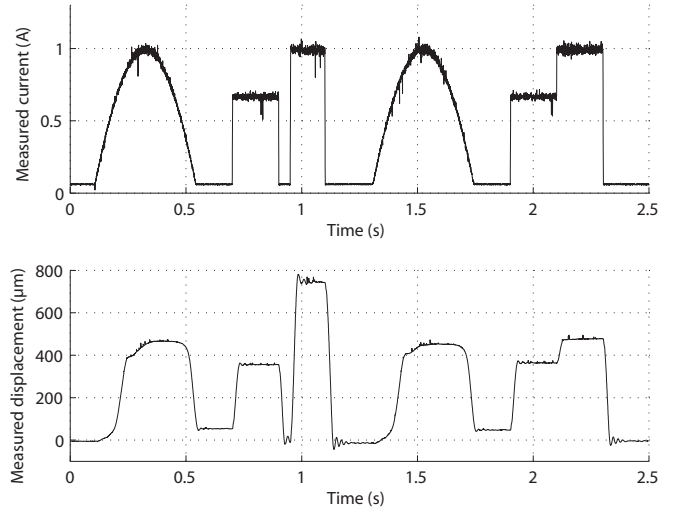


Fig. 4. Typical view of the difference between quasi-static and dynamic behaviour.

3) *Parameters identification*: we propose a method to identify the parameters x_{max}^S , x_{min}^S , A_{max} and A_{min} . An open loop test is built (see Fig. 5).

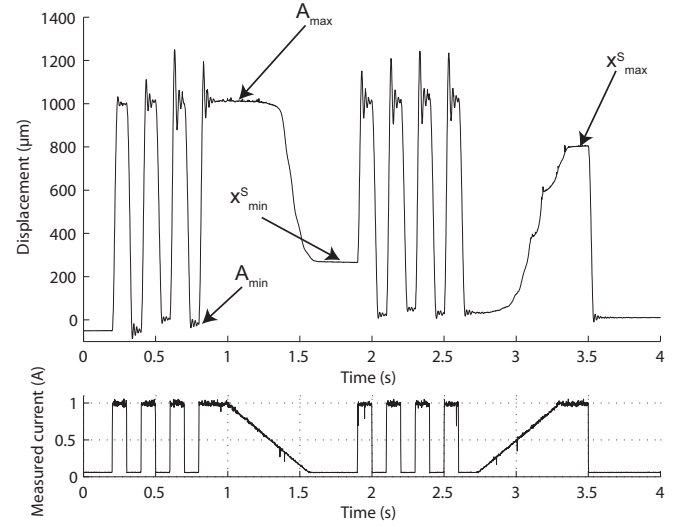


Fig. 5. Open loop test used for the identification of the parameters.

First, a series of maximum and minimum current values is applied in order to *reset* the MSMA sample (Memory points of hysteresis have to be erased as discussed in section III-C). A_{max} and A_{min} are identified. Then, a slow decrease of the current permits to obtain x_{min}^S . Finally another *reset* sequence followed by a slow increase permits to obtain x_{max}^S . Identified values are summarized in the following table:

$x_{max}^S = 573 \mu\text{m}$	$A_{max} = 1027 \mu\text{m}$
$x_{min}^S = 192 \mu\text{m}$	$A_{min} = -40 \mu\text{m}$

D. Energy exchange

A discussion about energy exchange in the system is presented here in order to design well-adapted control laws.

In the MSMA sample, we consider only the elastic part of the mechanical energy:

$$E_m = \frac{1}{2E}\sigma^2 = \frac{E}{2}(\varepsilon - \gamma z)^2 \quad (8)$$

For the load, kinetic energy E_c and gravity potential energy E_g are considered:

$$\begin{aligned} E_c &= \frac{m}{2}\dot{x}^2 \\ E_g &= mgx \end{aligned} \quad (9)$$

Heat losses resulting from the hysteresis into the MSMA sample Q_p and from the viscous damping of the system Q_v are taking into account:

$$\begin{aligned} Q_p &= \int_{z_0}^z \pi_f^* dz \\ Q_v &= \int_{t_0}^t f \dot{x}^2 dt \end{aligned} \quad (10)$$

The Fig. 6 (a) shows energy exchanges when the input changes slowly from 0 to its maximum value π_f^{mag} starting from the (0) point, representing the quasi-static mode. Dynamical effects can not be observed, therefore, the supplied energy is divided into heat losses into the MSMA sample (Q_{p1}) and gravity potential energy (E_{g1}). The Fig. 6 (b) shows energy exchanges when the maximum input $\pi_f^{mag} = \pi_{f,max}^{mag}$ is applied – dynamical mode – starting from the (0) point. Between point (0) and point (1), supplied energy is divided into gravity potential energy (E_{g1}), heat losses into MSMA (Q_{p1}) and energy due to dynamical effect (E_s). The latter can be divided into kinetic energy, elastic energy and heat losses by viscous damping. The path between points (1) and (2) is only possible if some energy is stored during the first sequence. Only a part of this storage energy (E_r : kinetic and elastic form) can be restored, because the heat Q_v is lost by viscous damping during all the sequence and corresponds to the difference between E_r and E_s .

IV. CONTROL STRATEGY

A. Hybrid control

A feedback control system was designed for the position control of the MSMA based actuator. We are currently working on different controllers to improve the stability and velocity of the control, nevertheless in this paper, we focus only on a new strategy designed to extend the displacement range of this actuator. In this paper, the tuning parameters of all the PID feedback controllers will be the same and tuned in a *trial and error* way ($K_p = 13.10^{-3}$, $T_i = 14.10^{-3}$ s and $T_d = 5.10^{-5}$ s). Some results using the simple control structure, i.e. the PID feedback controller without the hybrid strategy, are reported on the Fig. 8 (a) and the role of the new hybrid strategy will be to extend the displacement range above 600 μm and under 110 μm by using the dynamical specific properties of MSMA as seen in the previous sections. The idea of the new position control system looks like the swinging-up used to start the control of an inverted pendulum (see [6] for instance). In our system, the goal is to increase the maximum reachable strain by using inertial effects of

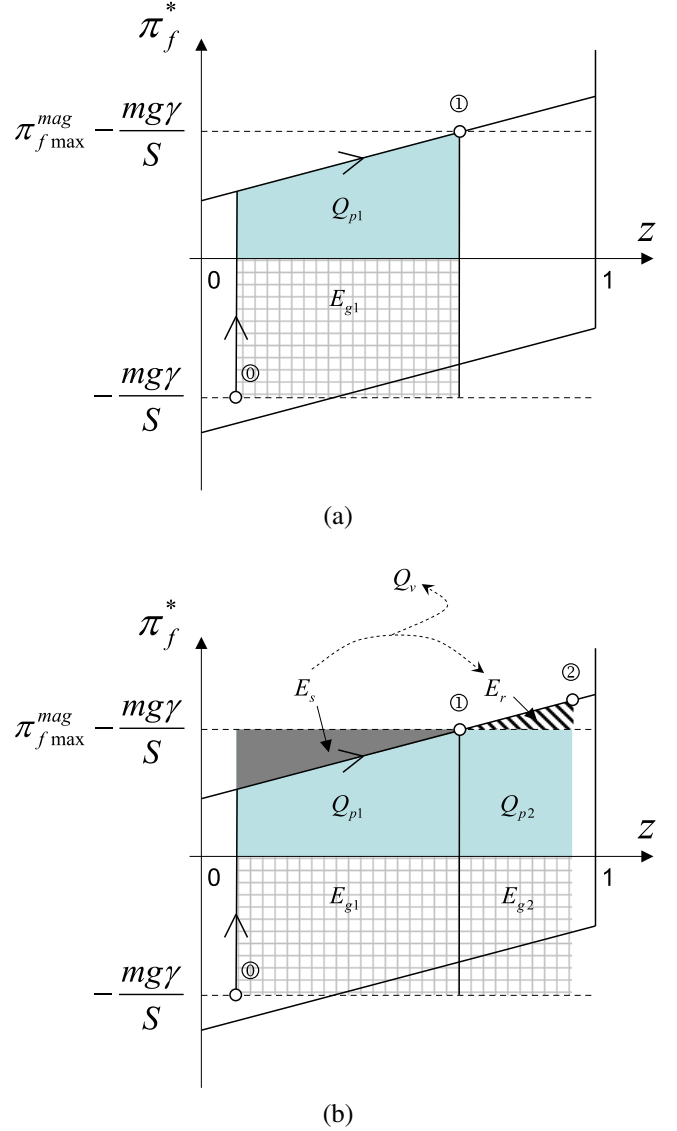


Fig. 6. Energetic point of view: (a) Quasi-static behaviour, (b) Dynamical behaviour.

the load. In periodic mode, this effect is just a resonance effect, but with a large hysteresis behaviour, it can be used to increase static gain of the system.

An hybrid control law was designed based on the position feedback control using the PID controller. The Fig. 7 is the general scheme of this hybrid control represented by a Petri net. At place p_0 , the PID based feedback control is used to obtain the control law of the current i . If transition t_1 is available, a run-up – storage – sequence is used to obtain larger displacement. At place p_1 minimum current value is imposed in order to quickly decrease displacement value, and at place p_2 maximum current value is set in order to quickly increase displacement value. When a higher displacement value is reached, the PID based feedback control is used again. In the reverse direction, the same scheme is used to obtain a smaller displacement with places p_3 and p_4 . Two

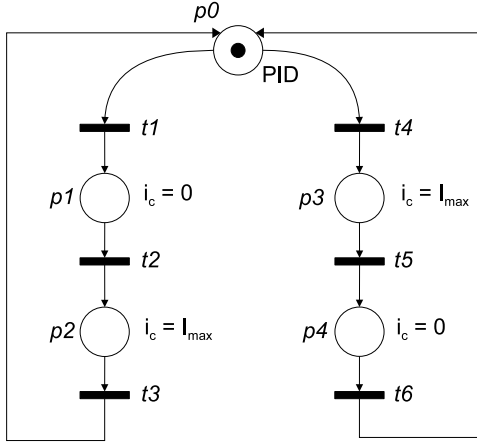


Fig. 7. Control strategy.

cases are discussed to obtain transition expressions $t1$, $t2$, $t3$, $t4$, $t5$ and $t6$. The first one is a method without model prediction: if maximum or minimum value of current is not enough to obtain desired displacement, then an energy storage sequence has to be applied. The second one is a method with a model prediction of the reachable displacement.

B. Without prediction switching

1) *Principle*: a test is made to obtain desired displacement value and if it is not the case, a run-up sequence is produced as an energy storage sequence. No model is used to obtain switching transitions:

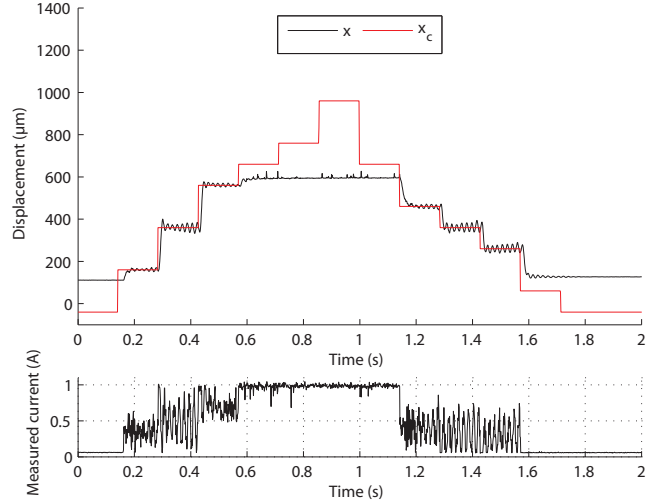
$$\begin{aligned}
 t1 &= (x < x_c) \cdot (i_c = i_{max}) \text{ during a delay } d1 \\
 t4 &= (x > x_c) \cdot (i_c = 0) \text{ during a delay } d1 \\
 t2 &= \text{delay } d2 \\
 t5 &= \text{delay } d2 \\
 t3 &= (x > x_c) \text{ during a delay } d3 \\
 t6 &= (x < x_c) \text{ during a delay } d3
 \end{aligned} \tag{11}$$

x_c is the set value (desired value) of displacement, x is the current measured displacement value. At the present time, three delay parameters $d1$, $d2$, and $d3$ have to be adjusted.

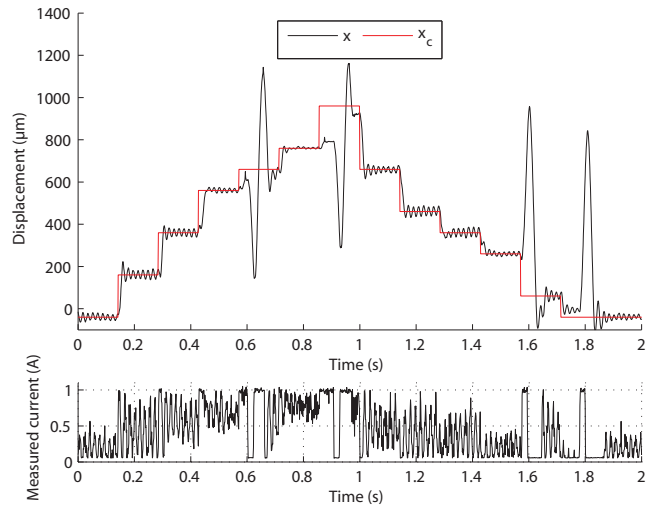
- $d1$ is the time required by the controller to consider that a run-up has to be set: a too small delay can force a run-up while it is not necessary, and a too large delay increases the response time of the closed-loop control. It depends on the PID controller tuning.
- $d2$ corresponds to the time required by the system to go backward: a too small delay does not generate enough displacement, and a too large delay increases the response time of the closed-loop control.
- $d3$ corresponds to the time required by the system to go forward: a too small delay does not generate enough displacement, and a too large delay increases the response time of the closed-loop control.

2) *Experimental results*: a comparison with the simple PID feedback control is drawn on Fig. 8 with $d1 = 50$ ms, $d2 = 20$ ms and $d3 = 20$ ms. The goal is reached: maximum

reachable displacement ($A_{max} - A_{min} = 1067\mu m$) is more than twice the reached displacement using the simpler feedback control ($490\mu m$).



(a)



(b)

Fig. 8. Experimental results: (a) simple PID based feedback controller, (b) hybrid controller without any model prediction.

C. Predictive switching

1) *Principle*: the model is used to predict if the desired displacement value is reachable. So, the model is used to obtain switching transitions:

$$\begin{aligned}
 t1 &= (x_c > x_{max}) \cdot (\dot{x}_c > 0) \\
 t4 &= (x_c < x_{min}) \cdot (\dot{x}_c < 0) \\
 t2 &= (x_{max} > x_c) \\
 t5 &= (x_{min} < x_c) \\
 t3 &= (x > x_c) \text{ during a delay } d3 \\
 t6 &= (x < x_c) \text{ during a delay } d3
 \end{aligned} \tag{12}$$

x_{min} and x_{max} are the minimum and maximum reachable displacement values using dynamical behaviour. When the measured displacement x is equal to x_{max}^S , no more displacement is reachable ($x_{max} = x_{max}^S$). But if x is equal to its absolute minimum value A_{min} , absolute maximum displacement A_{max} is reachable ($x_{max} = A_{max}$). In a first step, a linear function is chosen between these two extreme points and a similar function is chosen for x_{min} :

$$\begin{aligned} x_{max} &= \frac{x_{max}^S(x - A_{min}) + A_{max}(x_{max}^S - x)}{x_{max}^S - A_{min}} \\ x_{min} &= \frac{x_{min}^S(x - A_{max}) + A_{min}(x_{min}^S - x)}{x_{min}^S - A_{max}} \end{aligned} \quad (13)$$

$d3$ delay can be adjusted by the designer in order to increase robustness of the controller ($d3 = 10$ ms).

2) *Experimental results:* on the Fig. 9, an archetypal evolution shows active places of the hybrid controller with model prediction. Global results are drawn on the Fig. 10.

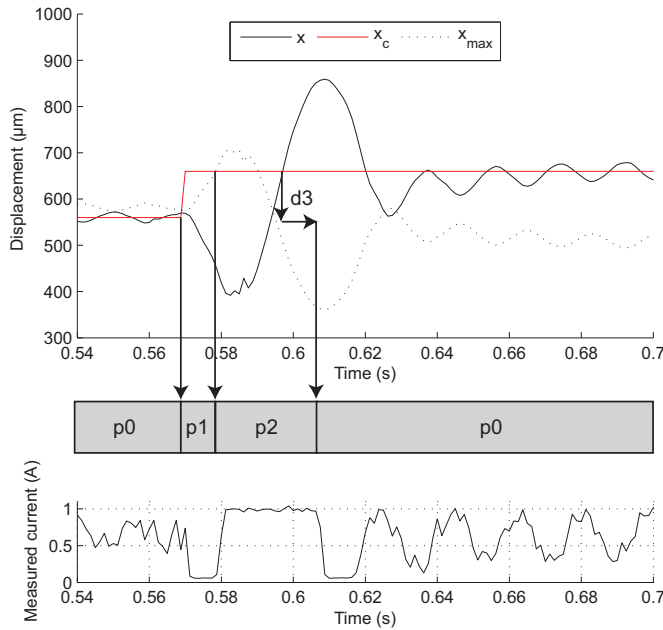


Fig. 9. Experimental results versus control places of the Petri net.

Hybrid controller without model prediction has lower performance in term of response time than the hybrid controller with model prediction. Nevertheless, due to the simpler inner loop modelling (especially at $t = 0.71$ s), the hybrid controller without model prediction can reach the set value without a run-up sequence when the hybrid predictive controller forces an unnecessary run-up sequence because of the error modelling. At this time, the first controller is more robust to error modelling but less optimal than the second one.

V. CONCLUSION AND PERSPECTIVES

We have seen in this paper that a good design of the control laws for a MSMA based actuator can increase performance in term of reachable static strain with a limited current amplitude input. Two original hybrid controllers have been

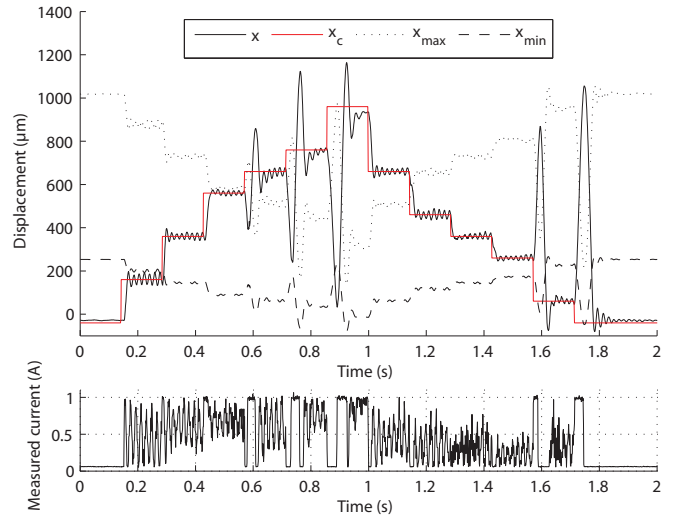


Fig. 10. Experimental results: hybrid controller with model prediction.

designed with the common goal to increase the reachable displacement range by using dynamical effects and hysteresis behaviour of the MSMA material. These laws can be used in all actuators containing a strong hysteretic behaviour if they are fast enough (with a high bandwidth). At the present time, in the run-up sequence, the maximum current is a constant but can be a function of measured and set displacement values to limits the overshoot. The predictive hybrid controller can be improved by using a more accurate model including more complicated inner loops of MSMA hysteresis. In these experiments, the tuning of the PID controller in the feedback control is not optimally chosen to obtain the best behaviour of the actuator when no run-up sequences are required but this can be easily improved by changing this tuning or the controller structure into a more efficient one. The large and fast actuation of this active material combined with a smart control permits to extend the number of available smart materials for micro-positioning and micro-robotics applications and opens new possibilities.

REFERENCES

- [1] K. Ullakko, J. K. Huang, C. Kantner, R. C. O'Handley, and V. V. Kokorin, "Large magnetic-field-induced strains in Ni_2MnGa single crystals," in *Applied Physics Letters*, vol. 69, no. 13, 1996, pp. 1966–1968.
- [2] R. D. James and M. Wuttig, "Magnetostriction of martensite," in *Philosophical Magazine A*, vol. 77, no. 5, 1998, pp. 1273 – 1299.
- [3] J. Tellinen, I. Suorsa, A. Jääskeläinen, I. Aaltio, and K. Ullakko, "Basic properties of magnetic shape memory actuators," in *8th international conference ACTUATOR 2002*, Bremen (Germany), 2002.
- [4] J. L. Pons, *Emerging Actuator Technologies: A Micromechatronic Approach*. John Wiley and Sons inc, 2005.
- [5] J. Y. Gauthier, C. LExcellent, A. Hubert, J. Abadie, and N. Chaillet, "Modeling rearrangement process of martensite platelets in a magnetic shape memory alloy Ni_2MnGa single crystal under magnetic field and (or) stress action," *Journal of Intelligent Material Systems and Structures*, vol. 18, no. 3, pp. 289–299, 2007.
- [6] K. J. Åström and K. Furuta, "Swinging up a pendulum by energy control," *Automatica*, vol. 36(2), pp. 287–295, 2000.